

Accepted Manuscript

On the colours and properties of building surface materials to mitigate urban heat islands in highly productive solar regions

Hassan Radhi, Essam Assem, Stephen Sharples



PII: S0360-1323(13)00319-3

DOI: [10.1016/j.buildenv.2013.11.005](https://doi.org/10.1016/j.buildenv.2013.11.005)

Reference: BAE 3556

To appear in: *Building and Environment*

Received Date: 30 August 2013

Revised Date: 21 October 2013

Accepted Date: 5 November 2013

Please cite this article as: Radhi H, Assem E, Sharples S, On the colours and properties of building surface materials to mitigate urban heat islands in highly productive solar regions, *Building and Environment* (2013), doi: 10.1016/j.buildenv.2013.11.005.

This is a PDF file of an unedited manuscript that has been accepted for publication. As a service to our customers we are providing this early version of the manuscript. The manuscript will undergo copyediting, typesetting, and review of the resulting proof before it is published in its final form. Please note that during the production process errors may be discovered which could affect the content, and all legal disclaimers that apply to the journal pertain.

On the colours and properties of building surface materials to mitigate urban heat islands in highly productive solar regions

Hassan Radhi ^{a,*}, Essam Assem ^b, Stephen Sharples ^c

^{a,*} Global Engineering Bureau, Manama, Bahrain.

^b Building and Energy Technologies Department, Kuwait Institute for Scientific Research, Kuwait

^c School of Architecture, University of Liverpool, United Kingdom

Abstract

An experimental study was conducted to assess the impact of building surface materials on urban heat islands (UHI) in highly productive solar regions. The study involved 32 surface materials commonly used in Bahrain and was performed during the summer period. The current work focuses on finishing materials at horizontal surfaces and examines the influence of material thermophysical and solar properties on their surface temperatures (T_s) and surface air temperatures (T_a) under clear sky conditions. A twofold assessment was deployed: first, experimental measurements of horizontal sample materials exposed to solar irradiation on a flat roof, and the second assessment involved full-scale experiments of roofs with different construction configurations. The analysis showed that the standard error of measurement in measured temperatures for all roofs was less than 3.5 °C, the standard error of mean was between 1.5 and 2.5 °C and the largest difference in standard deviations was 4 °C, indicating low bias. The range of errors in measurements was highest for the temperature of a dark porcelain roof. Overall, the errors were similar over all roofs. This work suggested that white and light colour materials were important to cope with surface UHI, while cool materials were beneficial and sensitive to highly productive solar regions, whereas materials with low heat storage capacity were significant as an atmospheric UHI reducer.

Keywords: Surface materials, surface temperatures, air temperatures, UHI

* Corresponding author: Hassan Radhi

e-mail address: h_radhi@yahoo.com

Tel: +93 34116633 - Fax: +973 17586142

1. Introduction

Properties and configurations of buildings have a significant impact on the thermal performance of urban environments. Such properties and configurations influence the development of urban heat islands (UHI), particularly when surface temperatures of exposed materials (T_s) become higher than their adjacent air temperatures (T_a) due to high solar irradiation – surface UHI. The increase in T_s affects the intensity of local and downwind air temperatures – atmospheric UHI, especially closer to the surfaces, due to various convective heat fluxes from the surfaces [1]. Increases in temperatures influence the quality of life as can be seen in the increased energy consumption for air-conditioning, elevated greenhouse gas emissions and compromised human comfort. Two recent studies [2, 3] examined the development of UHI phenomena in Bahrain and assessed their impact on the electricity consumption. Industrial regions were found to have higher UHI values due to various human activities including anthropogenic heat and sensible heat fluxes from urban surfaces such as roads and roofs. During the summer months, an increase of up to 10% in electricity consumption for air-conditioning occurred in those industrial regions.

Many sources assessed the role of urban surfaces in the development of UHI and proposed many solutions in order to reduce their impact on atmospheric and surface UHI. Some made use of vegetated systems [4-6] while others utilised white and cool materials. Past simulation analyses and test cell studies showed that the performance of materials under the sun was strongly correlated to the solar reflectance and the infrared emittance [7-10]. The former represents the ability of a material to reflect solar irradiation, while the latter relates to the ability of a material to release absorbed heat [11]. Materials with low values of reflectance or emittance would not

typically be considered cool. Similarly, a high reflectance value alone will not result in a “cool” material nor will a high emittance value alone. In order to accurately determine the “coolness” of any given materials, the solar reflectance index (SRI) can be a useful measure [12, 13]. It is a composite value of solar reflectance and thermal emittance calculated using the equation in ASTM E1980 [14]. In practice, SRI value for black surfaces would be close to 0 while for white surfaces, the SRI value would approach 100%. Normally, dark colour materials have a lower solar reflectance than light colour materials. Recently, however, some dark coloured materials have been developed with higher reflective values due to the use of cool coatings or some thermophysical treatments, and consequently have a high SRI. Therefore, cool materials are those coloured materials with high solar reflectance [15].

A recent study [16] proposed an international campaign to use cool materials in cities worldwide in order to reduce cooling energy and mitigate summer UHI. This technique is widely used for roofs, pavements and recently facades. Various techniques have been used to assess the performance of cool materials including laboratory and mathematical analyses. Such techniques are important for any accurate assessment. Experimental studies are also important to get realistic measurements. However, to show the intersection between surfaces and urban elements, full scale experiments are needed. For example, a laboratory and mathematical analysis of roof materials was conducted in Brazil to calculate the temperature that each material can reach when exposed to solar irradiation [17]. The analysis demonstrated that same coloured metal and ceramic materials reached different temperatures according to their radiative properties. Another laboratory analysis [18] reported quantitative values of radiative properties for a few types of materials and discussed which material characteristics affect such properties. These radiative properties were

assessed in a field experiments in Turkey to give a realistic assessment of material performance [19], while in Athens a field study in a very large application of cool pavements was carried out to reflect the performance of paving materials in real conditions [20]. This study documented the use of cool paving materials and showed that the use of cool pavements contributed to the reduction of the peak T_a and T_s during the summer.

The technique of cool roofs was used to measure the performance of facades in dense urban environments by using a reduced-scale of four street canyon rows [21]. The results showed that the cool coating preformed better than a standard coating. Although this study was able to give realistic measurements, the real interaction between vertical surfaces and building elements was explained by in-situ measurements in Malaysia [22]. This study came to the conclusion that heat storage capacity was the main influence contributing to the UHI impact. With more types of facade materials, a systematic analysis was carried out in Athens using two techniques, including in-situ measurements and experimental measurements [23]. The results showed that the temperatures during the summer period depend, first of all, on their orientation and secondly on their colour and other physical properties. A similar analysis was conducted in Kuwait [24], but this time with the use of simulation software. Orientation, colours and thermal properties such as thermal mass and thermal inertia were the main highlighted factors. Orientation defines the angle of incidence of the solar rays and the duration of insolation in addition to the hours of the day when it occurs, while colours determine the radiative properties of the surfaces. Thermal mass is the capacity of a material to absorb, store and release heat. This heat storage capacity can be determined by the specific heat capacity, density and thickness. It depends significantly on the thermal conductivity. The analysis

concluded that orientation, colours and thermal properties have a profound effect on the performance of surfaces, particularly for west wall orientations.

The current work assesses the performance of finishing materials on horizontal surfaces and examines the influence of material properties on their surface temperatures (T_s) and surface air temperatures (T_a) under clear skies. The focus is placed not only on the radiative properties but also on the role of heat storage capacity. This work conducted experimental studies in real conditions in order to get realistic measurements. It also performs full scale experiments to reflect the interaction between surfaces and urban elements, such as architectural masses and building structures.

2. Materials and methods

The materials and methods section first presents the study site and its climatic conditions. It then introduces the examined surface materials and case study roofs. It explains techniques of data collection and experimental measurements. This section finally evaluates errors and uncertainties in experimental measurements.

2.1. Study site and climatic conditions

In the current work, SITRA was selected. It is an industrial and residential urban island near Manama. Recent statistics show arid and semi-arid conditions: rainfall is low, irregular, seasonal and variable, relative humidity is also high, and temperatures are variable but high as shown in Fig.1. An important point to note is that the level of solar irradiation is similar in all areas of Bahrain, which experiences a high level of solar irradiation [25]. The highest monthly averages of direct, diffuse and normal solar irradiation are 585, 383 and 716 W/m² respectively. The maximum hourly values range from 820 to 1000 W/m² at noon in the month of June.

2.2. *Materials and samples*

The materials examined during the experimental study are usually applied on roofs, facades and external or paved floors in Bahrain. The focus of this work is placed on roof and floor surface materials. 32 samples of commonly used materials were examined. Some were with different sizes to examine the effect of mass and thickness. The samples were divided into five categories including: metal, felt, concrete, stone (e.g., sand stone, granite, marble, etc) and ceramic. Specifications were obtained from manufacturers, suppliers and contractors, in addition to data from major documents in the literature review [26, 27]. These specifications enabled the physical, thermal and radiative characteristics of materials to be analysed (Table 1). The SRI was calculated using the equation in ASTM E1980 [13]. Samples of the examined materials were arranged as shown in Fig. 2. They were fixed on to an insulated wooden board which was fixed on a flat roof with a 20 mm air gap using wooden stands to ensure that there was no contact between the roof and board to avoid thermal bridges.

2.3. *Full-scale experiments*

The need for more accurate and truthful measurements of T_s and T_a for roofs led to an extensive amount of T_s and T_a measurements. The selected roofs were located in the residential area of SITRA. Fig. 3 shows the location of study sites. The choice of these roofs was based on a number of criteria, which included:

1. Buildings to be within the same urban boundaries in order to ensure similar thermal and climatic conditions.
2. Buildings to have the same construction methods and structure materials.
3. Buildings with roofs constructed of common surface materials (e.g. lightweight screed, bituminous roofing felt, ceramic tiles, aluminium roof panels for service and garage areas, etc.) mainly with the flat roof system.

Table 2 illustrates the materials and compositions of the five examined roofs. They have different compositions and represent roofs with commonly used surface materials, including lightweight concrete screed, bituminous roofing felt, metal panels and light and dark colour ceramic tiles.

2.4. Data collection and experimental measurements

The measurements were conducted during the summer period, on days in June, July, August and September. These days were characterised by predominantly clear skies, elevated air temperatures and high levels of solar irradiation. Wind speed sensors and 4 simple data loggers of temperature and relative humidity were used. During the experimental study these loggers were placed in parallel to the horizontal surface of the board at 1.5 m distance. T_s was measured using a thermal camera/infrared thermometer (IR). Wind speed, relative humidity, T_a and T_s were measured simultaneously from 5:00 h to 24:00 h and recorded at 30 minute intervals. The 30 minute intervals were used due to the absence of smaller intervals of solar data collection.

Similarly, for the full-scale roof experiments the data loggers were placed in parallel to the horizontal surface of the roofs. The T_s of the selected roofs were measured using the IR. They were monitored from 5:00 h to 24:00 h and recorded at 30 minute intervals. In some cases, the measuring periods were extended to include 24 h. In order to ensure that recorded T_s were representative, the IR readings were taken at 4-5 measuring points representing different parts of the roofs. The measurements of T_a , relative humidity and wind speed were recorded at 1.5 m height from the roof surface. It is important to mention that solar irradiation was not measured in the study site, rather, readings from the Directorate of Meteorology in

Bahrain were utilised. Solar data were recorded at a distance of less than 10 km from the study site.

2.5. *Error and uncertainty in experiments*

Physical measurements are subject to a degree of error and uncertainty which, at best, can be reduced only to an acceptable level. It is common to classify errors in measurements into two broad categories, first, random errors, and second, systematic errors. The former is due to the accuracy of instruments which causes constant absolute (value) and relative (percentage) errors in all readings, while the latter is due to measuring skills. In other words, how well the instruments are used or how well the experiment conditions are controlled. Normally, more accurate instruments have a smaller range of error and uncertainty. In the current study, simple instruments with reasonable accuracy are used. The accuracy of the data loggers is ± 0.2 °C for temperature and $\pm 2\%$ for humidity, while the accuracy of IR is ± 3 °C. Based on such accuracy an assumption can be made that the actual measure lies either slightly above or slightly below the obtained readings. The range is the uncertainty of the readings taken. The standard error of measurement, standard error of mean and standard error of estimate are calculated from the measured parameter standard deviation and reliability estimate using the following formulae:

$$SEM = S \sqrt{1 - r_{xx}} \quad (1)$$

$$Sm = \frac{S}{\sqrt{n}} \quad (2)$$

$$SEE = Sy \sqrt{1 - r_{yx}^2} \quad (3)$$

where SEM = standard error of measurement, Sm = standard error of the mean, SEE = standard error of estimate, S = standard deviation, r_{xx} = reliability of the experiment (Cronbach alpha reliability estimate), n = number of observations, Sy = standard

deviation of the Y values in the regression analysis, ryx^2 = correlation squared of Y and X values in the regression analysis.

Table 3 shows the standard error of measurement with respect to T_s and T_a of the roofs. It is clear that the standard error of measurement in measured temperatures for all roofs is less than 3.5 °C, while the standard error of the mean is between 1.5 and 2.5 °C; the largest difference in standard deviations is 4 °C, indicating low bias. The range of errors in measurements is highest in T_s of dark porcelain roof. Overall, the errors are similar for all roofs. The error of regression which is the best estimate for the experimental uncertainty is used to obtain errors in T_s and T_a estimations. Regressing T_s onto T_a has led to a standard uncertainty in the intercept cases ranging from 1.0 to 2.5 °C. This range reduces to 0.02 °C in the case of slope. Probability and cumulative probability values are also calculated. The probability is an indication of the chance that a given event will happen, while the cumulative probability is an indication of the chance that two or more events will occur. Fig 4 shows the distribution of the relative errors for the monitored roofs. The ranges in the errors are similar for the five roofs for either T_s or T_a ; however, the error bias is slightly larger for T_s than for T_a .

3. Result and discussion

This section assesses the thermal performance of surface materials commonly used in Bahrain and examines the relationships between materials' properties and their T_s and T_a values under clear sky conditions.

3.1. Analysis of materials performance

Two main factors influence the thermal performance of surface materials: first, solar and ambient conditions, and second, thermal and radiative properties of materials. Fig. 5 shows hourly conditions during one day of measurement (21st June),

which is characterised by predominantly high air temperatures (32 to 43 °C), fluctuating relative humidities (15 to 65%), air velocities ranging from 2.4 to 8.7 m/s and high levels of normal solar irradiation with a peak value reaching 1000 W/m². In the case of properties, the sample materials under study have various values of specific heat capacity (420-1686 kJ/kgK), heat conductivity (0.41-45 W/mK), emissivities (0.85-0.95) and solar reflectance (19-88%).

The results from the monitoring experiments are illustrated in Fig. 6. For the different sample materials, the figure consists of the minimum and maximum T_s , in addition to T_a at the time of recording (t). It is important to note that the T_a in this case is not the T_a of the material in question; rather it is the T_a of the study site measured at 1.5 meters above the roof. A number of observations can be highlighted:

- (I) The solar irradiance heats material surfaces while wind speed results in a cooling effect. The lowest T_s values occur in the early morning at 5:00 h while the highest values occur in the afternoon between 13:00 h and 14:00 h. The effect of wind speed is obvious in the shift of maximum T_s from the noon period (the peak of solar irradiation) to the period between 13:00 h and 14:00 h. The difference in wind speed between the two periods is about 1.5 m/s. ΔT between minimum T_s and T_a in the early morning is small, varying from 0.5 to 5.5°C, but increases in the afternoon from 5.5 to 25.5 °C, particularly between 13:00 h and 14:00 h.
- (II) T_s and T_a of white colour materials are the lowest in each category. This is also applicable to light colour materials. Fig. 7 shows a thermal image in which the dark colour materials in each category, such as blue tiles and black and red granite, deliver higher T_s than others within the same category. This result is obvious when the T_s of white and yellow limestone are compared. The same scenario is repeated with the grey and orange composite aluminium with a SRI of

71 and 36 respectively. In addition, materials with reflective finishing layers such as glazed ceramic and coated concrete perform better than standard ceramic and concrete with and without standard coatings. Also, different materials with the same colour reached different T_s according to their heat storage capacity. The effect of heat storage capacity is obvious when different materials with an orange colour (e.g., orange aluminium, orange granite and orange ceramic tiles) are compared.

(III) Materials with high thermal mass (e.g., concrete, stone and granite, etc) generate higher heat storage and higher temperatures. For example, the concrete with its high heat storage capacity develops maximum T_s of 67.7 °C at 13:00 h, which is higher than the respective T_a by almost 25 °C. Another example is seen in the granite. It shows the highest difference between T_s and T_a that is close to 25.5 °C. This means that granite; particularly those with black and red colours, absorb more heat than other materials. Furthermore, the results of monitoring different sizes of materials indicate that materials with similar colours and properties and increased mass and thickness develop similar T_s of small mass and less thickness, in spite of that the amount of heat absorbed and stored within the volume is different. This analysis reflects the view of Levinson and Akbari [28] and Levinson et al [29] on the effects of composition and exposure on the solar reflectance of materials.

The outcome of the first step of the assessment is summarised in Fig 8. Overall, the lowest observed temperatures are for white and beige colour materials. The ceramic tile performs best followed by marble, stone, metal and concrete in descending order. The black and red granite are found to be the worst performers.

3.1.1 Analysis of full-scale experiments

The results of full-scale experiments are illustrated in Table 4. For the monitored roofs, the table consists of mean, minimum and maximum T_s in addition to T_a and time of recording (t). An important note to highlight is that the T_a in this case is that of the surface material in question. The tabled data show variation in the performance of roofs. The following briefly assesses the performance in each case.

3.1.2 Performance of concrete roofs

The examined concrete roof is a 52 mm Portland cement concrete screed floating over a water proofing layer which lies directly onto a concrete slab. There is a 300 mm air gap separating the slab and the internal gypsum ceiling. The surface layer is characterised by a low SRI (19) and moderate thermal conductivity (0.917 W/mK). Based on its properties, this roof absorbs, transfers and stores heat within its layers after sunrise from the solar irradiation hitting the surface. It heats up until it reaches thermal equilibrium. Fig 9 shows the performance of the concrete roof. The maximum T_a is 48.5 °C with mean and minimum values at 43.5 °C and 34.0 °C, respectively. The T_s is warmer than the corresponding T_a by 2.3 °C in the early morning (5.00 h). It reaches about 42.7°C at 7:00 h and is 4.1 °C higher than the T_a . At noon (12:00 h), the T_s rises to 59.3 °C which is higher than the T_a by 12.5 °C. The concrete roof develops maximum T_s of 62.5 °C at 13:30 h which is higher than the corresponding T_a by almost 13 °C. It can be noted that T_s increases during the middle of the day due to the high level of solar irradiation. With the decreasing level of solar irradiation, however, T_s drops steadily. After sunset (19:00 h), T_s remains warmer than T_a by 4.0 °C due to the heat stored in the subsurface. When the temperature of the adjoining air space becomes relatively lower due to some reasons such as an increase in wind speed, the stored heat in roof materials flows out and warms up T_a and consequently

develops atmospheric UHI warming. This scenario is obvious after midnight, when T_s decreases due to heat loss and the absence of solar irradiation, while T_a increases due to heat gain.

3.1.3 Performance of felt bitumen roofs

The examined felt bitumen roof is 4 mm bituminous roofing felt floating over a 50 mm cement screed which is painted with a primer layer. The screed lies directly on to a concrete slab. Fig. 10 shows the performance of this roof. The maximum T_a is 49.2 °C with mean and minimum values at 33.4 °C and 43.6 °C, respectively. The T_s of this roof is close to the T_a with less than a 0.5 °C difference in the early morning at 5:00 h. T_s reaches about 43.4 °C at 7:00 h and about 64.2 °C at 13:00 h, which is 13.5 °C higher than the corresponding T_a . It is clear that T_s increases rapidly during the middle of the day due to the high level of solar irradiation. With the decreasing level of the solar irradiation T_s drops steadily in the late afternoon. At 19:00 h, T_s drops close to T_a . Due to the moderate thermal conductivity and high specific heat, the screed and concrete slab below the felt enhances the heat storage capacity of the roof, which enables absorption of any heat from the solar irradiation. The T_s of such a roof, therefore, remains high at some parts of the night due to the storage of solar heat absorbed during the day. Similar to the concrete roof, the heat transfer scenario between the surface and air space is repeated where T_s decreases and T_a increases due to heat transfer.

3.1.4 Performance of metal roofs

The examined metal roof is aluminium-zinc-coated panels floating over a 50 mm extended polystyrene and fixed over a steel frame which is connected to a concrete structure. Fig. 11 shows that the maximum T_a is 44.5 °C at 13:30 h with

minimum and mean values at 34.0 °C and 40.5 °C, respectively. The T_s of metal panels are lower than the corresponding T_a in the early morning (5:00 h) and after sunset, but is higher under the sun. The T_s of the metal panels reach about 42.9 °C at 7:00 h and their value is 10.5 °C higher than T_a . Maximum T_s is warmer than T_a by 17 °C at 13:00 h. This roof is characterised by a high SRI (60-70%). Thus, it reflects a large amount of heat from incident solar irradiation. The illustration shows significant increases occur in T_s and T_a during the middle of the day. As the solar irradiation grows they increase and vice versa. The T_s drops slightly in the late afternoon to reach close to the air temperature at 19:00 h. The high thermal conductivity and small thickness represent negative factors for storing heat. Therefore, this type of roof loses heat faster than the others. At 20:00 h, T_s reduces to 33.0 °C or lower than T_a by almost 1.5 °C.

3.1.5 Performance of ceramic roofs

Two roofs, with two colours of ceramic tiles, are examined. The first is covered with beige porcelain (light colour roof). The second is covered with dark orange porcelain (dark colour roof). Porcelain is a type of ceramic but is harder, denser and more wear and damage resistant than other types. Both roofs are characterised by high heat storage capacities. Thus, they absorb and store a considerable amount of heat from the solar irradiation hitting their surface. However, this amount varies from one roof to another and depends largely on the SRI value of the surface material. Fig. 12 shows that the maximum T_a in both cases is 50.9 °C and 52.7 °C at 13:00 h for the light colour roof and dark colour roof respectively. The mean T_a values are within the range of 45.9 to 47.4 °C, while the minimum for both roofs is 36.3 °C. The two surfaces are warmer than the air by 1.5 and 2.5 °C at 7:00 h for the light colour roof and dark colour roof respectively. The T_s of dark colour roof

reaches a maximum of 50.3 °C, while the T_s of the light colour roof reaches a maximum of 43.3 °C. It can be noted that T_s and T_a are higher in the case of the dark roof, but the difference between them is larger in the case of the light colour roof. This difference becomes greater at 13:00 h where T_s of light colour roof reaches 60 °C, which is higher than T_a by 13.3 °C. The same scenario is repeated with the dark colour roof. T_s of the dark colour roof reaches about 68.9 °C with a 17 °C difference from T_a .

The properties of the two roofs show similar thermal conductivity and heat storage capacity, but a major difference in terms of SRI. The high SRI in the case of the light colour porcelain enables larger amounts of solar irradiation to be reflected. In contrast, the relatively low SRI in the case of the dark colour porcelain leads to the absorption of larger amount of heat from the incident solar irradiation which is then stored within the roof structure. This can be seen in the afternoon when the solar irradiation declines while the T_s of the roofs remain high. At night, where the level of solar irradiation is zero, the T_s of both roofs are still higher than T_a and reach almost 41 °C with a 5.0 °C difference from T_a . This difference is probably due to the storage of solar heat absorbed by the roof structure and materials including concrete and screed below the tiles. These results are very much in line with the findings of Kultur and Turkeri [19] who assessed the short-term and long-term solar reflectance performance of reflective roofs.

3.1.6 Overall performance of roofing materials commonly used in Bahrain

The comparison between horizontal surfaces is possible when they have similar conditions of experimental measurements. Fig. 13 compares the performance of the monitored roofs. The dark colour porcelain roof shows the highest maximum T_s of 69 °C and consequently the highest impact on the T_a at almost 52 °C. The felt roof

and concrete roofs also show high T_s values but with less impact on T_a . The dark colour porcelain and concrete roofs offer clear evidence of incremental temperature increases in the surrounding area because of their low SRI and high heat storage capacity. With the exception to the metal roof, the surface materials are characterised by low SRI and moderate thermal conductivity. Both are primarily properties of cool surface materials.

SRI, on the one hand, affects the T_s of surfaces as well as the subsurface temperatures. Surface materials with a low SRI absorb more heat energy, creating a hotter temperature and warmer subsurface temperatures due to the more heat transferred into the roof structure and subsurface. The absorbed heat, stored within the structure, flows out to the surrounding area and warms up the ambient T_a . For example, the dark and light colour porcelain have similar thermal conductivities and heat storage capacities, but the light colour porcelain shows lower maximum T_s values and a lower impact on the T_a . The SRI of the light colour porcelain is relatively higher than that of the dark colour porcelain. This means that the amount of absorbed heat from solar irradiation at a particular time is lower in the case of the lighter colour. Another example is seen in the metal roof with its high SRI. The metal roof shows a moderate impact on T_s and T_a when compared to other roofs. This result is very much in line with other findings in this field [20] which indicate that the higher SRI of a material then the lower are T_s and T_a .

On the other hand, the heat storage capacity plays a significant role in the thermal performance of roofs. Moderate conductivity and high specific heat lead the surface materials and overlaid concrete slabs to not only store a large amount of heat during the day, but also to release a large amount of heat after sunset. The thermal conductivity and heat storage capacity of some roofing materials such as the metal

panels enable the surface to have a lower T_s than conventional materials such as concrete and porcelain roofs (3 to 9 °C difference) during the day. In addition, the amount of heat released by the overlaid layers of the porcelain and concrete roofs are significantly higher than that released by the overlaid layers of the metal roof due to larger reservoirs of heat stored in the subsurface. This analysis reflects the view of Asaeda and Ca [30] relating to heat storage in pavements and its effect on the atmosphere.

4. Conclusion and future work

This study has measured the thermal performance of a number of surface and roofing materials commonly used in Bahrain. Experimental measurements were first conducted and then full-scale experiments were carried out. An error analysis of measurements showed that the standard error of measurement in measured temperatures for all roofs was less than 3.5 °C, while the standard error of the mean was between 1.5 and 2.5 °C, whereas the largest difference in standard deviations was 4 °C, indicating low bias. The analysis of material performance showed that the surface temperatures (T_s) and surface air temperatures (T_a) during the summer period were depending largely on colour, thermophysical properties and radiative properties of the materials. The T_s temperatures of the light colour materials were lower than those of the dark colour materials. At the peak of solar irradiation, the highest observed temperature was for black granite at 68 °C, while the lowest observed temperature was for the white ceramic at 45 °C. However, the same coloured materials, such as orange metal, orange granite and orange ceramic, reached different T_s (59, 63 and 53 °C respectively) according to their SRI and heat storage capacity. Materials with high thermal mass, such as concrete and granite, generated higher values of heat storage and temperatures. The concrete, with its high heat storage

capacity, could develop maximum T_s of 67.7 °C, which was higher than the respective T_a by almost 25 °C; this difference reached almost 25.5 °C in the case of granite. Based on the first steps of assessment, this study concludes that the ceramic tile performs best, followed by marble, stone, metal and concrete in descending order. The granite is found to be the worst performer.

To reflect the interaction between surfaces and urban elements, this study assessed the performance of five real roofs. They represented roofs with surface materials that are common in Bahrain, including lightweight concrete, roofing felt, metal sheets and ceramic tiles. The performance of these roofs was mainly influenced by the SRI of the surface materials and the heat storage capacity of the overlaid layers. Roofing materials with high SRI and low heat storage capacity, such the coated metal panels, were able to reflect a large amount of solar irradiation and consequently produced a lower impact on T_a with a value of 44 °C. In contrast, roofing materials with a low SRI and high heat storage capacity, such as the dark colour porcelain, produced the highest maximum T_s with a value of 69 °C and, consequently, had the highest impact on the T_a , which reached 52 °C. The findings of this paper can be summarised as follows:

- 1- The lowest T_s and T_a at any hour during the day are developed by the white colour materials such as white ceramic, white marble, followed by light colour materials such as beige porcelain.
- 2- Glazed ceramic tiles and coated concrete are cooler than conventional ceramic and concrete with and without a standard coating.
- 3- The light colour porcelain performed best followed by the aluminium panels, lightweight concrete screed and felt bitumen roofing materials in descending order.

The findings introduced in this work can help design teams to improve the thermal performance of future buildings and mitigate UHI impacts. This work showed

that T_s and T_a were affected by ambient conditions and material properties. Introducing methods to examine the relationship between these factors and T_s and T_a can be a valuable and convenient method for assessing the impact of building materials on the UHI in regions of high solar radiation such as Bahrain.

References

- [[1] U.S. Environmental Protection Agency, 2012. Reducing urban heat islands: compendium of strategies-urban heat island basics.
<<http://www.epa.gov/hiri/resources/pdf/BasicsCompendium.pdf>>.
- [2] Radhi H, Fikry F, Sharples S. Impacts of urbanisation on the thermal behaviour of new built up environments – a scoping study of the urban heat island in Bahrain. *Landscape and Urban Planning* 2013, 113: 47– 61.
- [3] Radhi H, Sharples S. Quantifying the domestic electricity consumption for air-conditioning due to urban heat islands in hot arid regions. *Applied Energy* 2013, 112: 371–380.
- [4] Cheng CY, Cheung KKS, Chu LM. Thermal performance of a vegetated cladding system on facade walls. *Building and Environment* 2010, 45: 1779-1787.
- [5] Alexandri E, Jones P. Temperature decreases in an urban canyon due to green walls and green roofs in diverse climates. *Building and Environment* 2008, 43:480 – 493.
- [6] Sheweka SM, Mohamed NM. Green facades as a new sustainable approach towards climate change. *Energy Procedia* 2012, 18: 507–520.
- [7] Taha H. Modeling the impact of large-scale albedo changes on ozone air quality in the south coast air basin. *Atmospheric Environment* 1997, 31 (11): 1667-1676.
- [8] Taha H. Urban climates and heat islands: albedo, evapotranspiration, and anthropogenic heat. *Energy and Buildings* 1997, 25: 99-103.
- [9] Taha H, Douglas S, Haney J. Mesoscale meteorological and air quality impacts of increased urban albedo and vegetation. *Energy and Buildings* 1997; 25: 169-177.
- [10] Akbari H, Konopacki SJ. The Impact of Reflectivity and Emissivity of Roofs on Building Cooling and Heating Energy Use. *Proceedings of the Thermal Performance of the Exterior Envelopes of Building VII*. December 6-10, 1998. Clearwater Beach, FL.
- [11] Marceau ML, VanGeem MG. Solar reflectance of concretes for LEED sustainable sites credit: Heat island effect. *Research & Development Information*. Portland Cement Association 2007.
<www.concretethinker.com/Content/Upload%5C446.pdf>.

- [12] Alchapar NL, Correa EN, Canton MA. Solar reflectance index of pedestrian pavements and their response to aging. *Journal of Clean Energy Technologies* 2013, 1 (4): 281-285.
- [13] Parker DS, McIlvaine JER, Barkaszi SF, Beal DJ, Anello MT. Laboratory testing of the reflectance properties of roofing material. FSEC-CR670-00. Florida Solar Energy Center, Cocoa, FL 2000.
< <http://www.fsec.ucf.edu/~bdac/pubs/CR670/CR670.htm>>
- [14] Akbari H, Levinson R, Berdahl P. "ASTM Standards for Measuring solar Reflectance and Infrared Emittance of Construction Materials and Comparing their Steady-State Surface Temperatures". Energy and Environment Division, Ernest Orlando Lawrence Berkeley National Laboratory. Presented at the American Council for Energy Efficient Economy Summer Study, August 1996.
- [15] Akbari H, Berdahl P, Levinson R, Wiel S. Cool color roofing materials. Lawrence Berkeley National Laboratory Berkeley 2006, CA. Report no: 94720
- [16] Akbari H, Matthews HD. Global cooling updates: reflective roofs and pavements *Energy and Buildings* 2012, 55: 2-6
- [17] Prado R, Ferreira F. Measurement of albedo and analysis of its influence the temperature of building roof materials. *Energy and Buildings* 2005, 37, 295-300.
- [18] Berdahl P, Bretz SE. Preliminary survey of the solar reflectance of cool roofing materials. *Energy and Buildings* 1997, 25 (2): 149–158
- [19] Kultur S, Turkeri N. Solar reflectance performance of roof coverings in Istanbul, Turkey. *World Renewable Energy Congress* 2011, pp: 1978-1985.
- [20] Santamouris M, Gaitani N, Spanou A, Saliari M, Giannopoulou K, Vasilakopoulou K, Kardomateas T. Using cool paving materials to improve microclimate of urban areas - design realization and results of the flisvos project. *Building and Environment* 2012, 53: 128-136.
- [21] Doya M, Bozonnet E, Allard F. Experimental measurement of cool facades' performance in a dense urban environment. *Energy and Buildings* 2012, 55: 42–50.
- [22] Din MF, Dzinun H, Mohanadoss P, Chelliapan S, Noor ZZ, Ossen DR, Iwao K, Investigation of heat impact behavior on exterior wall of building material at urban city area. *Civil Environment Eng* 2012, 2(2):1-6.
- [23] Bougiatioti F, Evangelinos E, Poulakos G, Zacharopoulos E. The summer thermal behaviour of "skin" materials for vertical s in Athens, Greece as a decisive parameter for their selection. *Solar Energy* 2009, 83: 582–598.
- [24] Assem EO. Correlating thermal transmittance limits of walls and roofs to orientation and solar absorption. *Energy and Buildings* 2011, 43: 3173–3180.
- [25] Alnaser WE, Al-Attar R. Simple models for estimating the total\ diffuse\direct and normal solar irradiation in Bahrain. *Technical note. Renewable Energy* 1999, 18: 417-434.

- [26] CIBSE. Environmental design, CIBSE guide A. Chartered Institution of Building Services Engineers, London, UK, 2006.
- [27] ASHRAE. ASHRAE Handbook of Fundamentals. Atlanta, GA: the American Society of Heating, Refrigerating and Air-Conditioning Engineers 2013.
- [28] Levinson R, Akbari H. Effects of Composition and Exposure on the Solar Reflectance of Portland Cement Concrete. Publication No. LBNL 48334. Lawrence Berkeley National Laboratory, 2001.
- [29] Levinson R, Berdahl P, Akbari H. Lawrence Berkeley National Lab Pigment Database: characterizing the solar spectral radiative properties of conventional and cool pigmented coatings. Lawrence Berkeley National Laboratory 2009. <<http://coolcolors.lbl.gov/LBNL-Pigment-Database/database.html>>.
- [30] Asaeda T, Ca VA. Heat Storage of Pavement and its Effect on Atmosphere. Atmospheric Environment 1996, 30 (3): 413-427.

List of Illustrations

Figure 1	Climatic elements of Bahrain
Figure 2	Samples of examined materials
Figure 3	Locations for field observations in SITRA.
Figure 4	Distribution of systemic errors
Figure 5	Hourly climatic and solar condition during the day of measurement
Figure 6	Analysis of material samples
Figure 7	Thermal image of studied materials
Figure 8	Performance of material samples
Figure 9	The performance of concrete roofs
Figure 10	The performance of roofing felt
Figure 11	The performance of metal roofs
Figure 12	The performance of ceramic roofs
Figure 13	A comparison between the five roofs
Table-1	Physical, thermal and radiative characteristics of materials
Table-2	materials and composition of examined roofs
Table-3	Errors of experimental measurements
Table-4	Results of full-scale experiments

Material	Symbols	Dimensions (mm)	Conductivity W/m.k	Density Kg/m ³	Specific heat (kJ/kg.K)	Infrared Emittance	Solar Reflectance (%)	SRI (%)
Composite Alum-Gray	Al-GY	150 x150 x 6	45	7680	420	0.89	71	87
Composite Alum-Orange	AL-OR	150 x 150 x 6	45	7680	420	0.89	36	39
Aluminium-zinc panel	AL-ZP	150 x 150 x 5	45	7800	480	0.87	57	68
Bituminous roofing felt	R-FLT	150 x 150 x 4	0.85	2400	1000	0.87	23	21
Concrete-grey	C-GY	200 x 200 x 52	0.719	2050	890	0.90	20	19
Concrete-cool coating	C-CO	200 x 200 x 50	0.41	2050	840	0.90	70-88	86
Interlock-Red	IN-RD	200 x 100 x 80	0.960	2000	840	0.85-0.90	55	64
Interlock-Yellow	IN-YW	200 x 100 x 80	0.960	2000	840	0.85-0.90	58	68
Artificial Stone-Beige	ST-AR	200 x 200 x 45	0.840	1700	800	0.90	45	52
Stone Chipping-White	ST-CH	200 x 200 x 40	1.74	2240	1686	0.90-0.93	49	67
Sandstone-Light brown	ST-BN	200 x 200 x 20	1.836	2200	712	0.90-0.93	45	52
Limestone-White	ST-WT	200 x 200 x 25	1.500	2180	720	0.90-0.93	55	65
Limestone-Yellow	ST-YW	200 x 200 x 25	1.500	2180	720	0.90-0.93	45	52
Granite-Black	GR-BK	120 x 120 x 20	3.49	2880	840	0.85-0.95	19-25	15
Granite-Gray	GR-GY	120 x 120 x 20	3.49	2880	840	0.85-0.95	25-30	23
Granite-Orange	GR-OG	120 x 120 x 20	3.49	2880	840	0.85-0.95	33-35	34
Granite-Brown	GR-BN	120 x 120 x 20	3.49	2880	840	0.85-0.95	29-35	28
Granite-Beige	GR-BG	120 x 120 x 20	3.49	2880	840	0.85-0.95	44-54	49
Granite Red	GR-RD	120 x 120 x 20	2.900	2650	900	0.90-0.93	19-24	18
Marble-Black	ML-BK	120 x 120 x 20	2.770	2600	880	0.90-0.93	20-25	19
Marble-White	ML-WT	120 x 120 x 20	2.900	2750	880	0.84-0.93	55	63
Porcelain-Orange	PR-OG	300 x 150 x 10	0.80	2400	920	0.85-0.95	30-35	30
Porcelain-Brown	PR-BN	300 x 150 x 10	0.80	2400	920	0.85-0.95	27-30	26
Porcelain-Beige	PR-BG	300 x 150 x 10	0.80	2400	920	0.85-0.94	42-54	46
Ceramic-Gray	CR-GY	300 x 300 x 7	0.80	1700	840	0.85-0.90	23-25	20
Ceramic-Orange	CR-OG	300 x 300 x 5	0.80	1700	840	0.85-0.95	30-35	30
Ceramic-White	CR-WT	300 x 300 x 7	1.2	1700	840	0.85-0.94	72-77	88
Ceramic-Blue	CR-BL	300 x 300 x 7	0.80	1700	840	0.85-0.95	22-40	19
Ceramic-glazed orange	CR-GOR	200 x 200 x 5	0.80	2500	840	0.88-0.95	32-45	34
Ceramic- glazed green	CR-GGN	200 x 200 x 5	0.80	2500	840	0.88-0.95	35-50	38
Ceramic-Brown	CR-BN	300 x 300 x 7	0.80	1700	840	0.85-0.95	27-30	26
Ceramic-Beige	CR-BG	300 x 300 x 7	1.3	1700	840	0.85-0.94	42-54	46
Ceramic- glazed-Beige	CR-GZ	300 x 300 x 5	1.3	1700	840	0.85-0.94	70-77	85

Solar absorptance = 1-solar reflectance

Table 1: Physical, thermal and radiative characteristics of materials

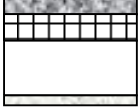

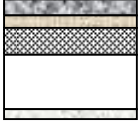

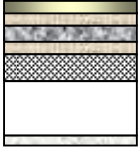
Roof	Construction	Layers	Thickness (m)	Conductivity (W/m.k)	Density (Kg/m ³)	Specific heat (kJ/kg.K)
Aluminum panel		Aluminum panel	0.005	45	7800	480
		Ext. polystyrene	0.050	0.020	1000	1700
		Air gab	0.300	0.027	1.13	1005
		Gypsum board	0.012	0.420	1200	840
Felt bitumen		Roofing felt	0.004	0.85	2400	1000
		Pained screed	0.050	0.22	1490	0.26
		Concrete slab	0.150	1.31	2200	920
		Air gab	0.300	0.027	1.13	1005
		Gypsum board	0.012	0.420	1200	840
Concrete screed		Concrete screed	0.052	0.719	2050	890
		water proofing	0.004	0.152	1121	1510
		Concrete slab	0.150	1.31	2200	920
		Air gab	0.300	0.027	1.13	1005
		Gypsum board	0.012	0.420	1200	840
Porcelain-Beige		Light porcelain	0.006	0.80	2400	920
		Mortar	0.025	0.719	2050	840
		Sand screed	0.050	1.818	1700	800
		Concrete slab	0.150	1.31	2200	920
		Air gab	0.300	0.027	1.13	1005
Porcelain-Orange		Dark porcelain	0.006	0.80	2400	920
		Mortar	0.025	0.719	2050	840
		Sand screed	0.050	1.818	1700	800
		Concrete slab	0.150	1.31	2200	920
		Air gab	0.300	0.027	1.13	1005
		Gypsum board	0.012	0.420	1200	840

Table 2: Surface materials and compositions of examined roofs

	Surface temperature T_s (°C)				Surface air temperature T_a (°C)				Uncertainty in T_a estimation				Uncert in
	Mean	STD	Sm	SEM	Mean	STD	Sm	SEM	Intercept	Uncer	Slope	Uncert	expt data
Concrete	51	8.4	1.9	1.4	43	4.5	1.0	0.7	16.60	1.67	0.52	0.03	1.24
Metal	49	9.8	2.2	1.6	41	3.6	0.8	0.6	23.26	0.93	0.36	0.02	0.83
Felt	52	11.2	2.5	1.8	43	5.3	1.2	0.8	19.41	1.31	0.46	0.02	1.24
Light porc	48	8.7	1.6	2.0	44	6.8	1.2	1.2	9.63	2.37	0.73	0.05	2.08
Dark porc	53	13.1	2.4	3.0	44	7.5	1.4	1.3	15.19	2.32	0.56	0.04	2.62

Table 3: Errors of experimental measurements

	Mean Ts	Min Ts	Ta	ΔT_{\min}	Time:	Max Ts	Ta	ΔT_{\max}	Time:
Roofing material	(°C)	(°C)	(°C)	(°C)	24:00	(°C)	(°C)	(°C)	24:00
Aluminium-zinc panels	47.4	33.0	34.3	1.3	5:00	61.5	44.5	17.0	13:00
Felt bitumen roofs	52.9	33.9	33.4	0.5	5:00	64.4	49.2	15.0	13:00
Light weight concrete screed	51.0	36.4	34.1	2.3	5:00	62.0	48.5	13.5	13:30
Porcelain-Beige	49.4	36.5	35.2	1.3	23:00	60.0	50.9	9.1	13:00
Porcelain-Orange	56.7	38.1	36.6	1.6	23:00	68.9	51.9	17.0	13:00
Min Ts, Max Ts and Ta are absolute temperature									
ΔT_{\min} : The temperature difference between min Ts and Ta & ΔT_{\max} : The temperature difference between max Ts and Ta at time of recording									

Table 4: Results of full-scale experiments

'Research highlights'

- Surface and air temperatures are depending on colour and thermal and radiative properties.
- Lowest temperatures are developed by white colour materials, followed by light colour materials.
- Ceramic performs best, followed by marble, stone, metal and concrete in descending order.
- Black and red granite are the worst performers.
- Roofing materials with high thermal mass generate higher heat storage and temperatures.

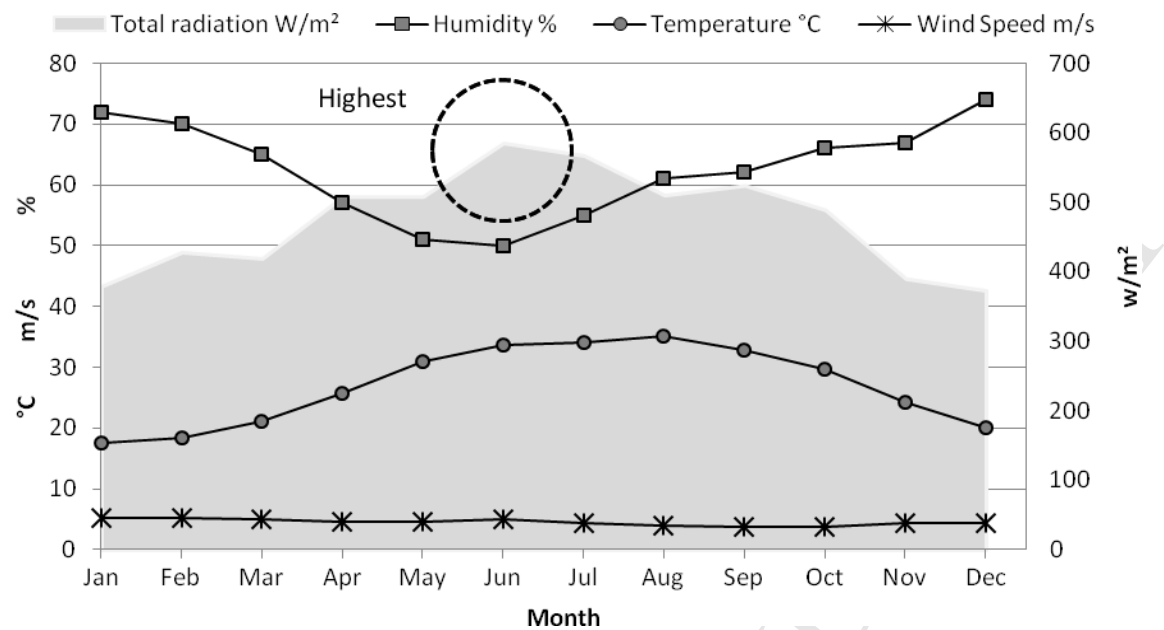


Fig. 1 Climatic elements of Bahrain



Fig. 2: Samples of examined materials



Fig. 3: Locations for field observations in SITRA.

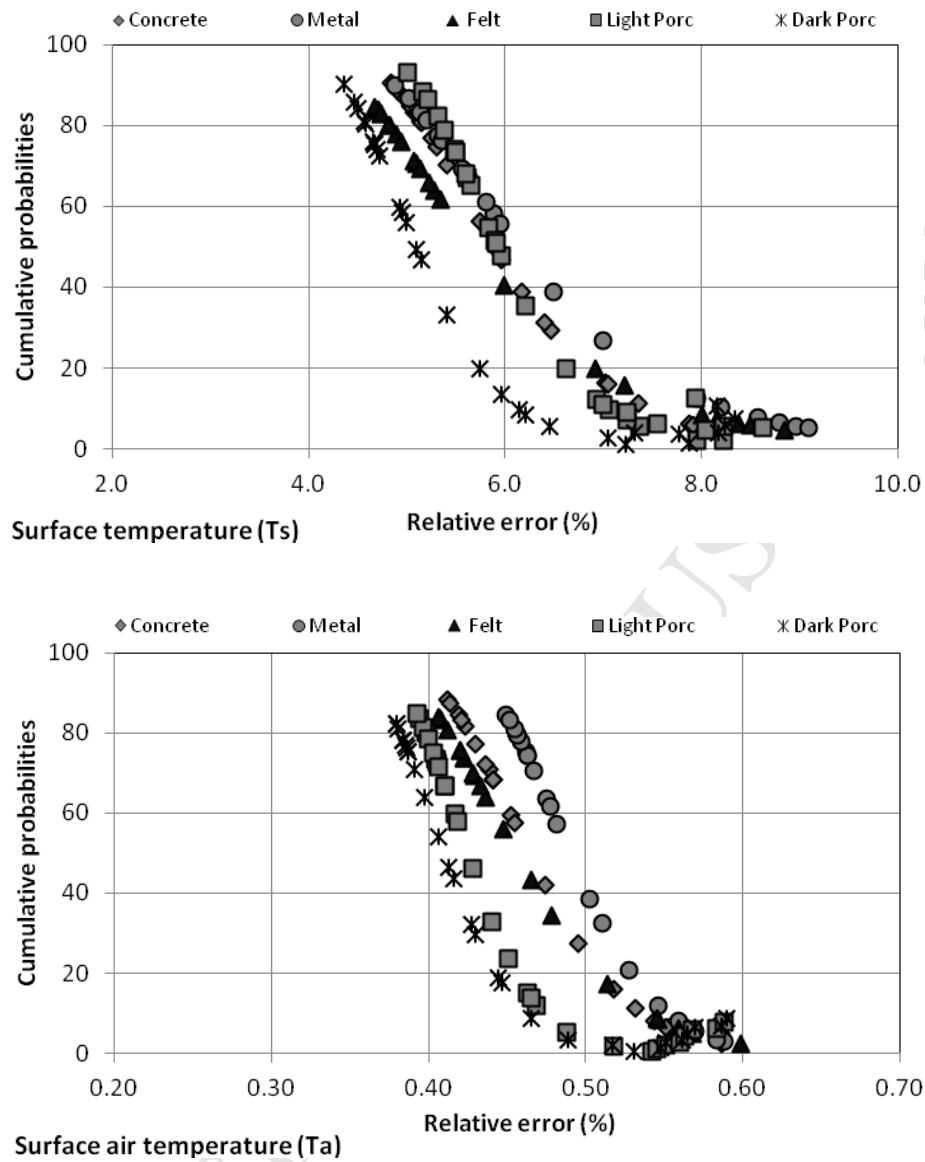


Fig. 4: Distribution of systemic errors

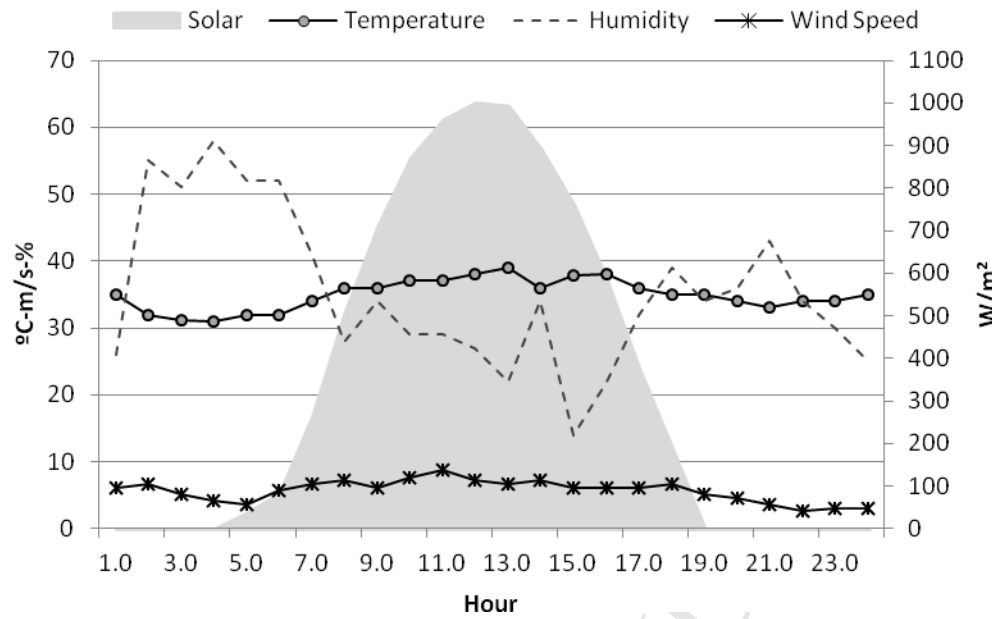


Fig. 5: Hourly climatic and solar conditions during the day of measurement

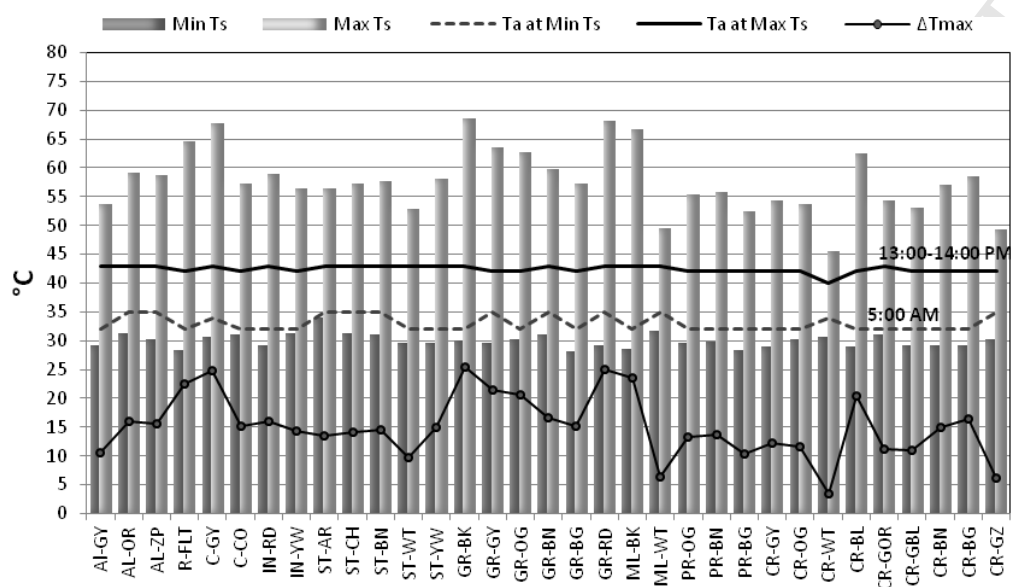


Fig.6: Analysis of material samples

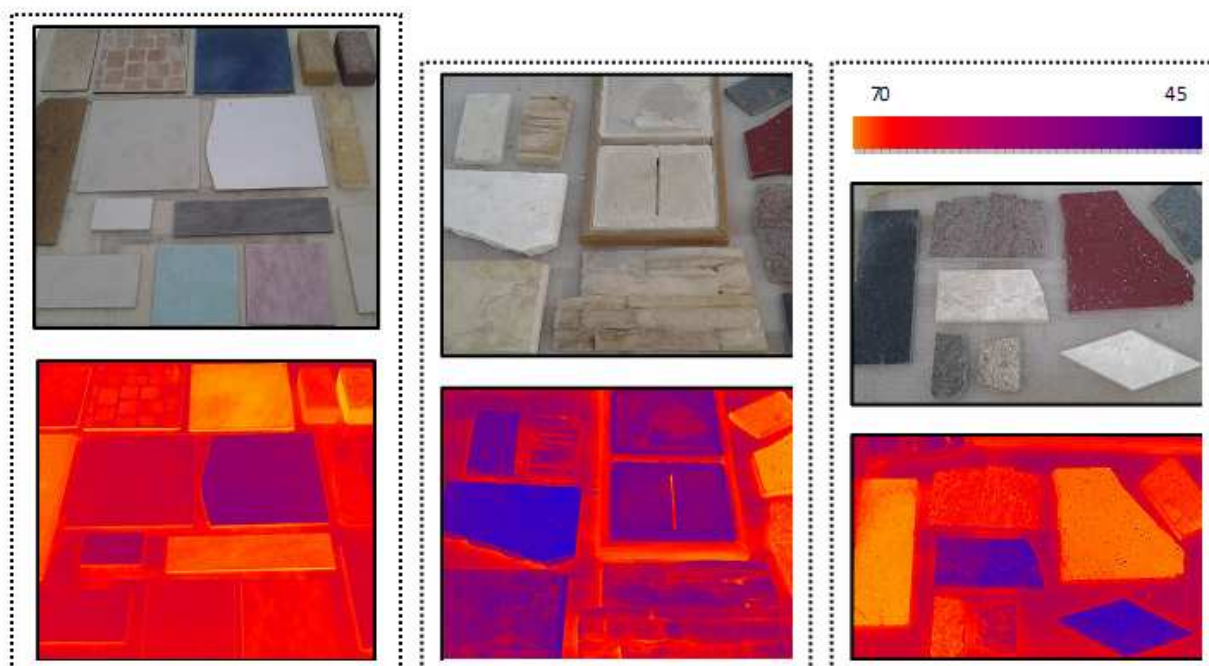


Fig. 7: Thermal image of some studied materials

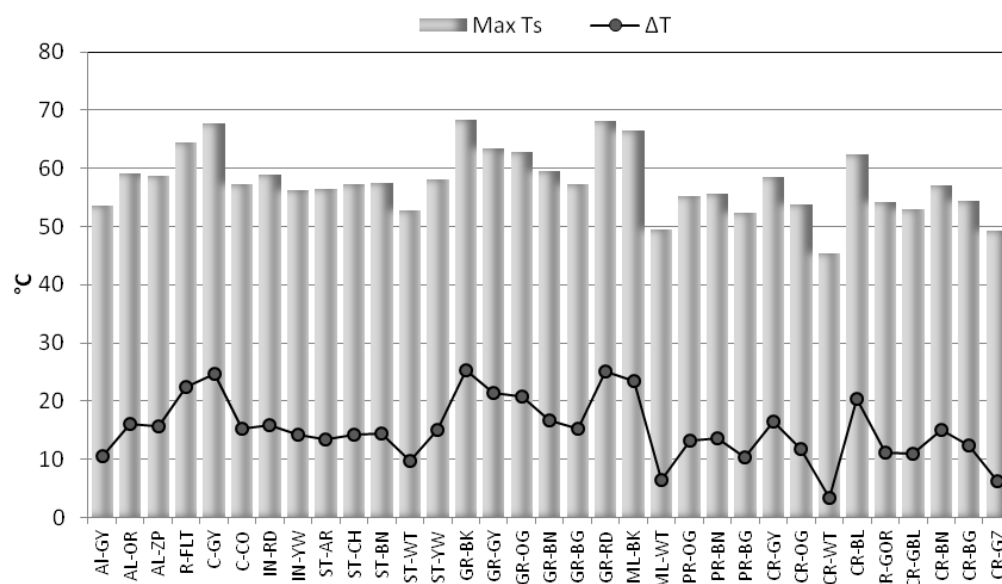


Fig. 8: Performance of material samples

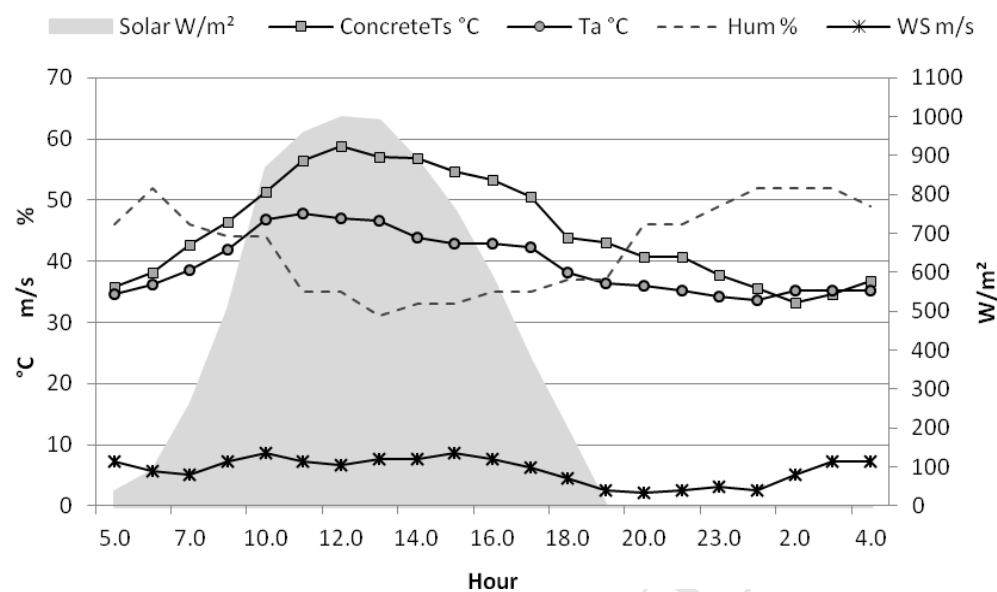


Fig. 9: The performance of concrete roofs

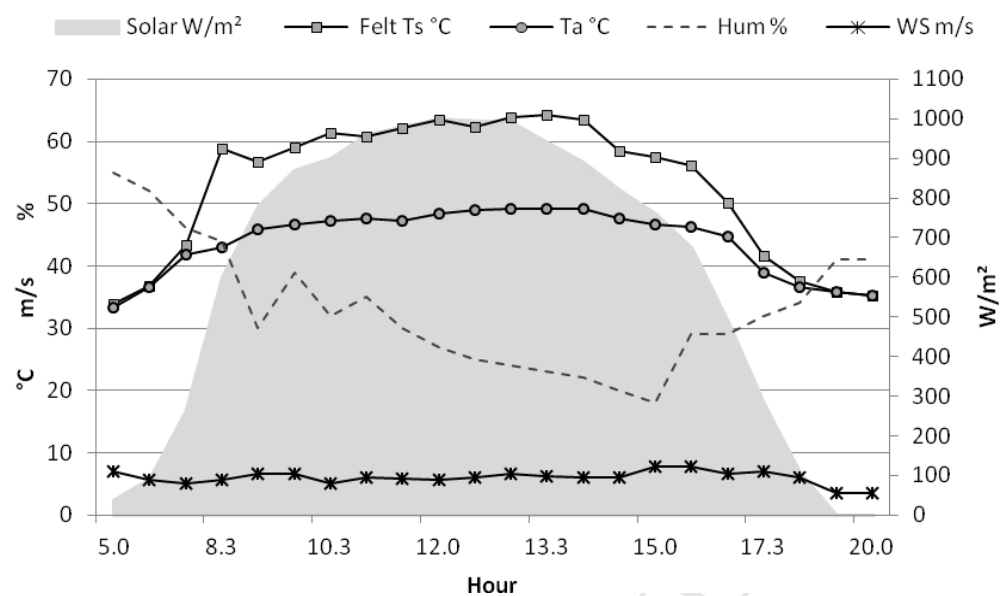


Fig. 10: The performance of roofing felt

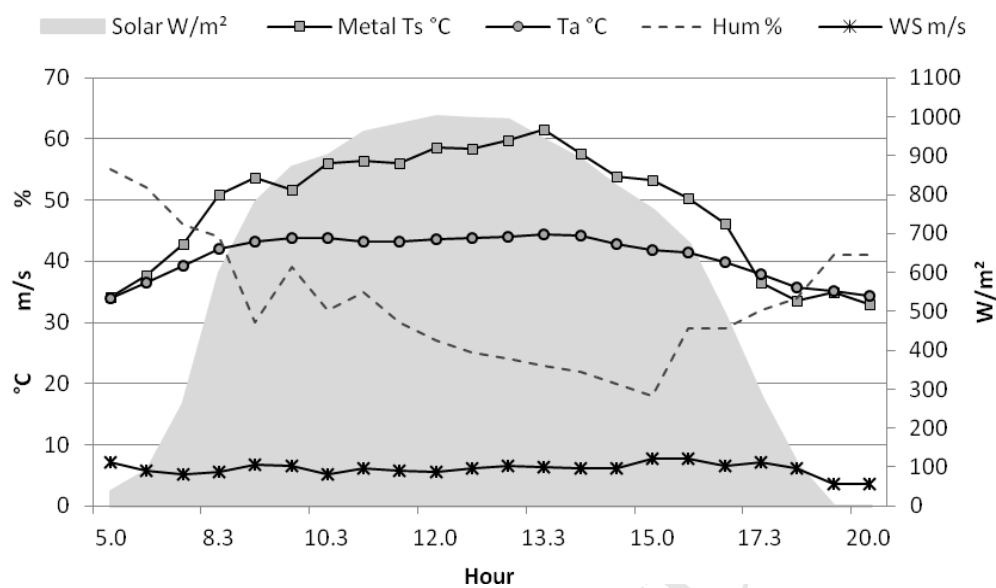


Fig. 11: The performance of metal roofs

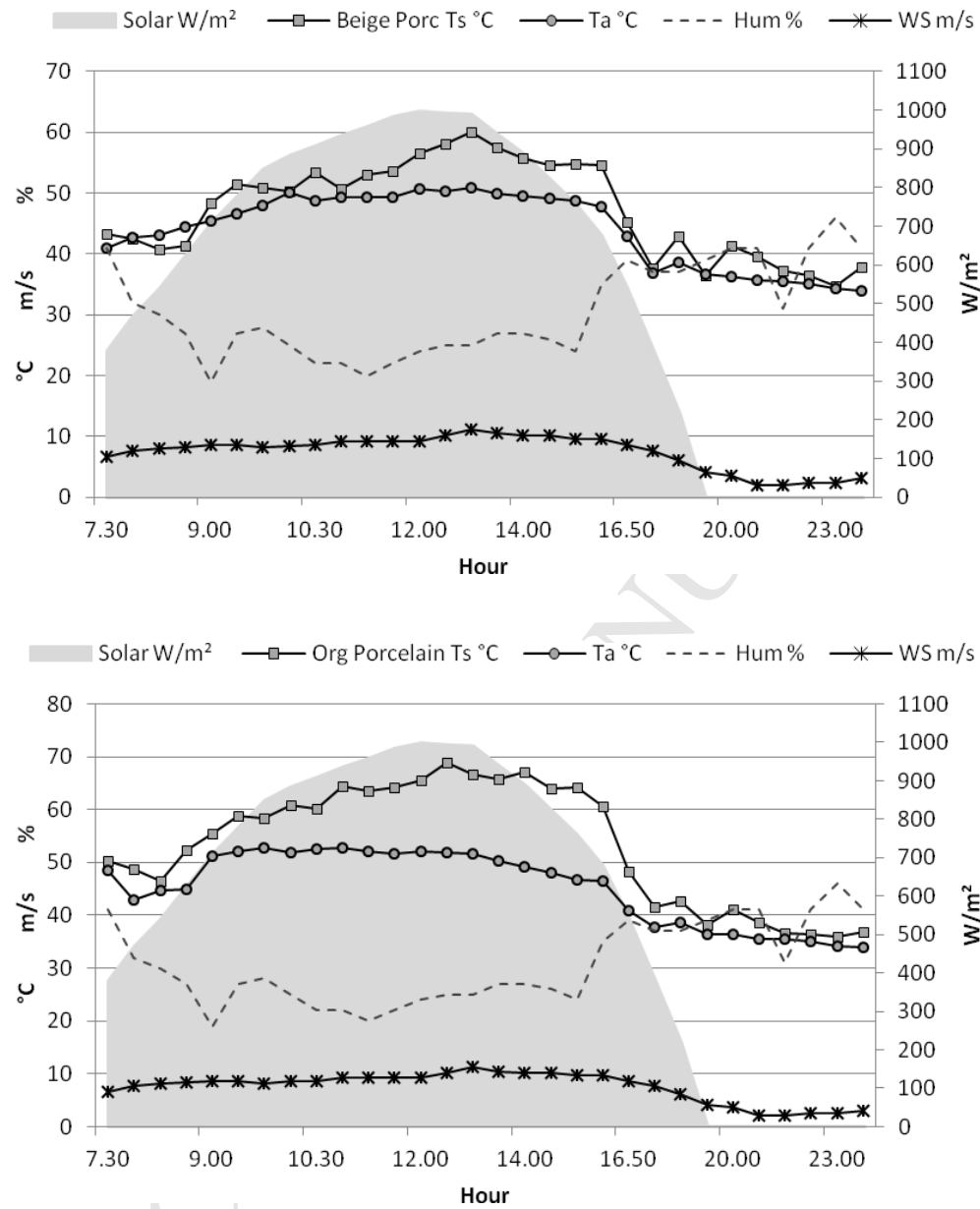


Fig. 12: The performance of ceramic roofs

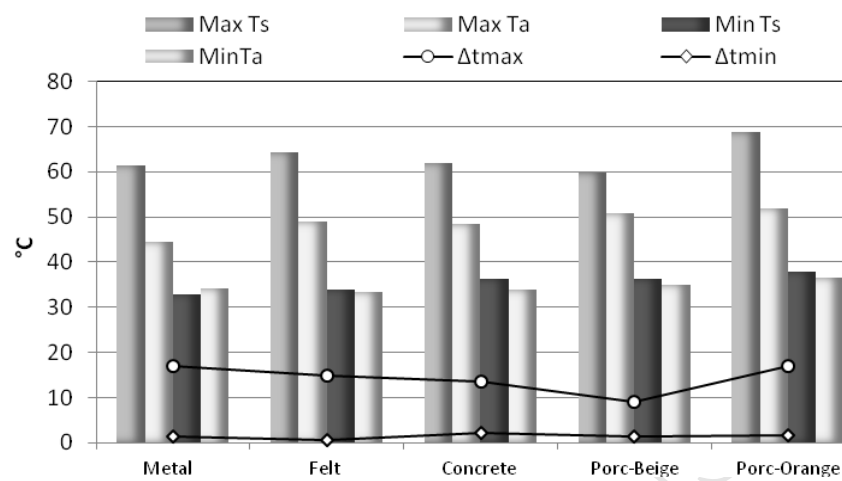


Fig. 13: A comparison between the five roofs